

Optical Relays for Imaging Scintillators

Robert M. Malone^{a*}, Stuart A. Baker^a, Daniel K. Frayer^a, Todd J. Haines^a,

Kevin T. Joyce^b, Morris I. Kaufman^a, Paul K. Manhart^a

Katherine L. Walters^a, Eloisa Zepeda-Alarcon^a

^aNevada National Security Site, Transformational Diagnostic and Imaging,
2900 East Rd., Los Alamos, NM USA 87544; ^bLawrence Livermore National Laboratory,
Livermore, CA USA 94550

ABSTRACT

Cygnus is a dual beam high-energy radiographic x-ray source. Ten years ago, three large zoom lenses were assembled to collect images from 200 mm x 200 mm square scintillators. The zoom capability allows zooming down to a 60 mm x 60 mm picture from the scintillator. Current radiographic imaging needs now require larger 270 mm x 270 mm square scintillators and the capability to use both 92 mm x 92 mm and 62 mm x 62 mm CCD cameras, and a new lens design to meet these needs. This zoom lens incorporates 11 elements and is designed to be telecentric. It images a scintillator emitting light peaking at 435 nm, so special glass types are required for the lens elements. Much larger elliptical pellicles are needed to deflect the scintillator light out of the x-ray path into the lens. The optical axis of the imaging system must be colinear with the x-ray axis. Two scintillators are positioned in each of two Cygnus x-ray axes, for a total of four scintillators and four lens systems. An optional configuration will be shown, enabling two lens systems imaging opposite sides of a single scintillator, for a total of four lenses and two scintillators. Although this configuration has advantages, it suffers from crosstalk. Care must be taken to analyze the anti-reflection coatings applied to all the elements in the imaging chain, including the CCD array and its vacuum window. The evolution of our Cygnus radiographic systems over the last two decades will be discussed.

Keywords: optical design, x-ray radiography, optical alignment, optical tolerance

1. INTRODUCTION

The Cygnus Dual Beam Radiographic Facility^{1,2} consists of two identical radiographic sources at 2.25 MeV. Each rod-pinch x-ray source is aimed at a test object from a different angle. Each source produces a 700-micron diameter x-ray spot size, with 4 Rad at 1 m, in a pulse of 50 ns FWHM. X-ray collimators define the beam axis. This radiographic facility is in an underground tunnel test area at the Nevada National Security Site (NNSS). The sources were developed to produce high-resolution images on subcritical tests that are performed at NNSS. Subcritical tests are single-shot, high-value events. The test objects can be different sizes and a variety of different CCD cameras are available. A zoom lens design accommodating magnification changes that would enhance the Cygnus facility was set up in 2013. Three zoom lens systems were built, with the third zoom system available to other users for future R&D work.

The Cygnus source is a rod-pinch diode with a 2.3 MeV bremsstrahlung endpoint energy and a 700-micron spot that provides high-resolution radiographs. This pulsed x-ray source is used to probe dynamic experiments at selected times. Figure 1 shows the x-ray beam (magenta color) going through a collimator, passes the bulkhead wall (shown in gray) and through the experiment vessel windows to interact with the material of interest. Timing of the dynamic experiment with respect to the firing of Cygnus is carefully planned for the different requirements of the experiment. As the x-rays exit the experiment vessel and reach the x-ray scintillators, the x-rays are converted to visible photons. The photons then travel through the lens systems, hit the camera CCD chips, and get recorded.

*malonerm@nv.doe.gov; phone 1 505 663-2014; fax 1 505 553-2003; nnss.gov

Initial imaging started in 2004 using only the Camera 1 system. A specially designed LINOS lens system would relay light from a 150 x 150 mm scintillator onto a 50 mm square CCD camera. The CCD camera was vacuum coupled to this LINOS lens and provided no magnification adjustments. To accommodate magnification changes, a zoom lens system^{3,4} was setup in 2013. This allowed adjusting the field of view at the scintillator from 60 x 60 mm up to 200 x 200 mm. The zoom lens also allowed using either a 50 mm square CCD camera or a 62 mm square CCD camera. The 50 mm square CCD camera provided 2K pixel resolutions. The 62 mm square CCD camera provided 4K pixel resolutions.

In Figure 1, it was decided to use both imaging systems together. X-rays hit the first scintillator producing radiographic image 1, pass through a mylar pellicle and into a second scintillator producing radiographic image 2. The two recorded images are at different magnification. However, enhanced statistics allowed higher density dynamic ranges of the test object to be recorded. Figure 1 shows only one of two Cygnus x-ray sources. There is a second x-ray source that passes through the vessel at a 60-degree angle to the first axis.

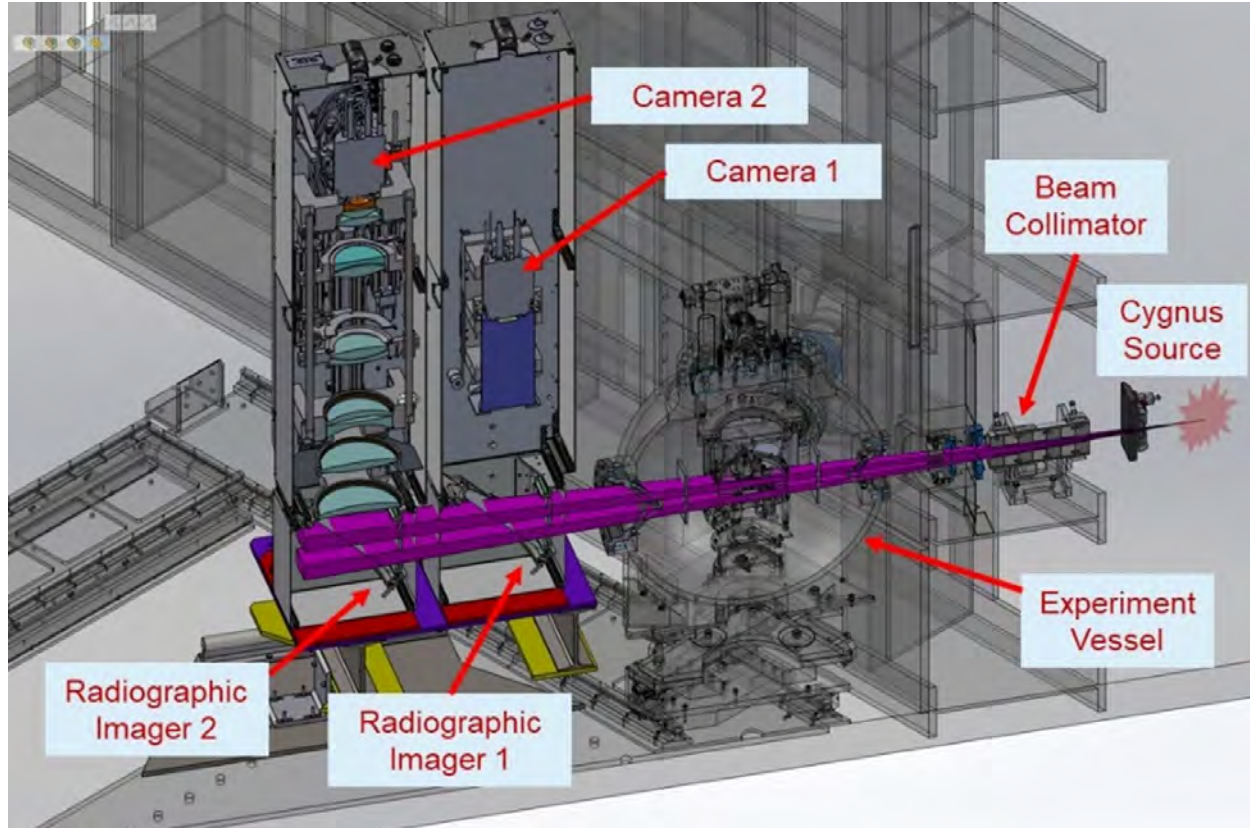


Figure 1. One of two imaging axes at the Cygnus x-ray facility. Each Cygnus axis is recorded onto two imaging systems.

2. DUAL SCINTILLATOR APPROACH FOR INCREASED DYNAMIC RANGE

It is of interest to the Assessment Sciences Stockpile Stewardship program to understand and model the dynamics of features of a wide range of areal mass values. To meet this need, we designed, tested, and fielded a new combined imaging system at Cygnus, expanding the areal mass dynamic range over approximately five orders of magnitude. A dual scintillator, two-camera approach allows simultaneous optimization in different portions of the x-ray spectrum. The dual scintillator design relies on using a thin scintillator in the “front” upstream imaging system and a thick scintillator in the “back” downstream imaging system. The material and thickness of the thin scintillator are selected such that low-energy x-rays of the x-ray spectrum are absorbed by it. The thick scintillator is designed to capture the high-energy tail of the source x-ray spectrum. A 20 mm thick LYSO detector array is ideal for this purpose.

The dual scintillator imaging configuration shown in figure 1 has been a great success. The thin P43 scintillator provided information from the light ejecta material generated in the experiment, and the 20 mm thick LYSO scintillator provided information about the dense material dynamic behavior. Many advantages of having a dual imaging system at Cygnus have been identified, and development work in this topic is ongoing.

3. EVOLUTION OF IMAGING SYSTEMS

Initially, a LINOS lens system was used with a 2K CCD camera. This was later upgraded to use a 4K CCD camera. This LINOS lens was vacuum coupled to the CCD camera. Its field of view was limited to only 150 mm. In 2013, two zoom lenses named Cygnus Zoom Lens Systems (CZLS), were installed at an x-ray facility (CYGNUS) to collect images with a 200 mm x 200 mm field of view at the scintillator detector plane^{3,4}. This was a large improvement from the original Cygnus LINOS lenses that had a field of view of only 150 mm x 150 mm and collected ~56% less light. The zoom capability of the CZLS allows zooming down to a 60 mm x 60 mm region at the scintillator, but current radiographic imaging needs for upcoming subcritical experiments require a larger 270 mm x 270 mm field of view and the capability to use a more modern 92 mm x 92 mm, 6k x 6k pixel CCD camera, shown in Figure 2c. More stringent requirements on the resolution at the object location and accuracy in the areal mass are required to be measured. The new Better Effective Field Focus Imaging Lens (BEFFI) design presented here will meet these needs.

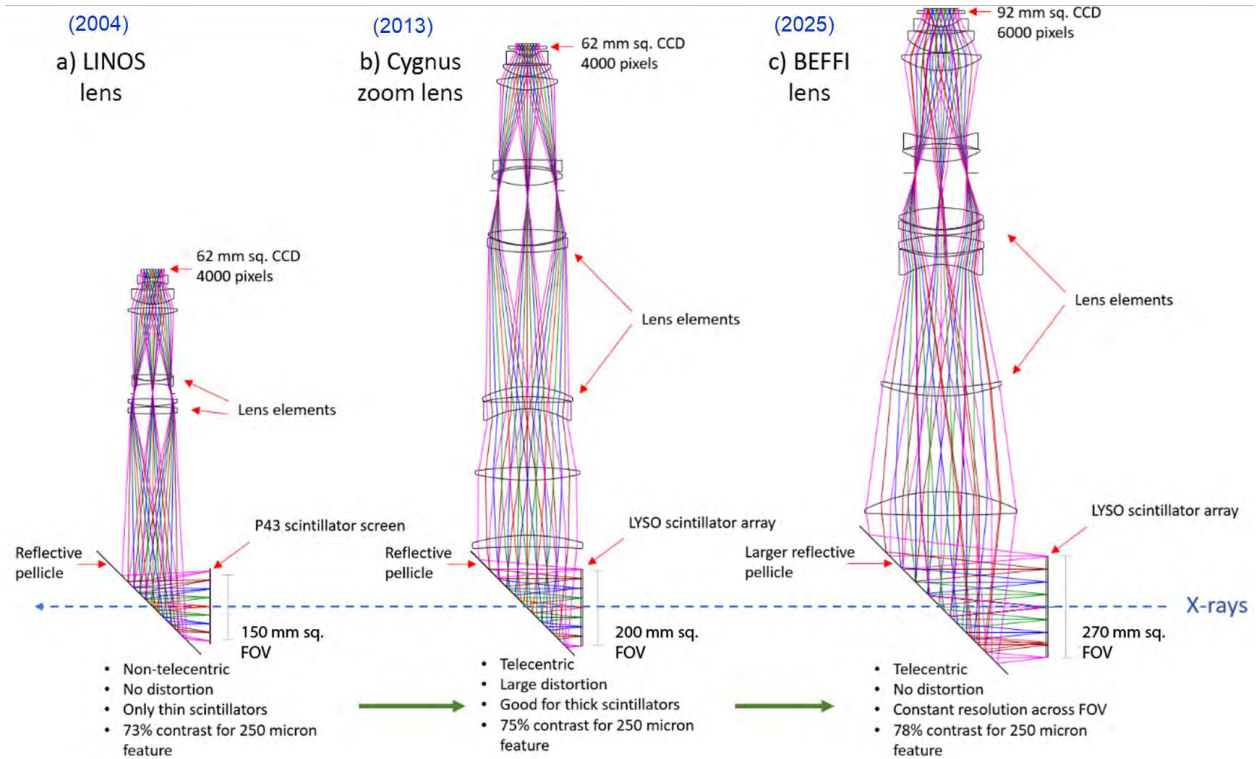


Figure 2. Evolution of Cygnus imaging systems over time.

Figure 2a shows the LINOS lens with 150 mm x 150 mm field of view. This lens is not telecentric so only thin scintillators are recommended to be used in this system. It is now used with a 62 mm x 62 mm 4k x 4k pixel CCD, but it was originally designed for a 50 mm x 50 mm 2k x 2k pixel camera, so the lens system does not cover the whole chip size of the larger 4K camera. In Figure 2b, the CZL lens has a 200 mm x 200 mm field of view. Designed to be used with thicker scintillators, the CZL lens is a telecentric lens and is also designed to use a higher resolution camera than the LINOS. Large distortion of the CZL at the edges of the field of view must be corrected for in analysis. In Figure 2c, the new BEFFI lens provides a larger 270 mm x 270 mm field of view, operates with better resolution, and has no distortion in the edges of the field of view. It also has a more homogeneous contrast of features across the field of view.

In figure 2, the lens systems are shown with scintillator plane, reflective pellicle, lens elements and camera CCD at the image plane. Multicolor rays are shown passing through the system simulating photons transmitting through the lens.

4. SCINTILLATOR TILING

The current zoom lens design (Figure 2b) required the recording of 60 mm to 200 mm diameter object features from a tiled 200 mm square LYSO scintillator. Large LYSO scintillators cannot be fabricated easily. So, 3 tiles were cemented together to form the larger 200 mm square scintillator. Figure 3 shows the FOVs of the LINOS lens, Cygnus zoom lens, and the new BEFFI lens, as well as the larger scintillator detector panel that is required for this larger 270 × 270 mm FOV. The larger scintillator detector panel is comprised of seven 200 × 66 mm rectangular LYSO monolithic crystals and four-corner squares of the same material. The outlines of the scintillator “tiles” are shown in green in Figure 3. This larger FOV will provide data that can better constrain and validate models of the material of interest. The larger FOV will also allow calibration objects to be imaged in situ with the dynamic experiment, providing information necessary to improve accuracy of image analysis.

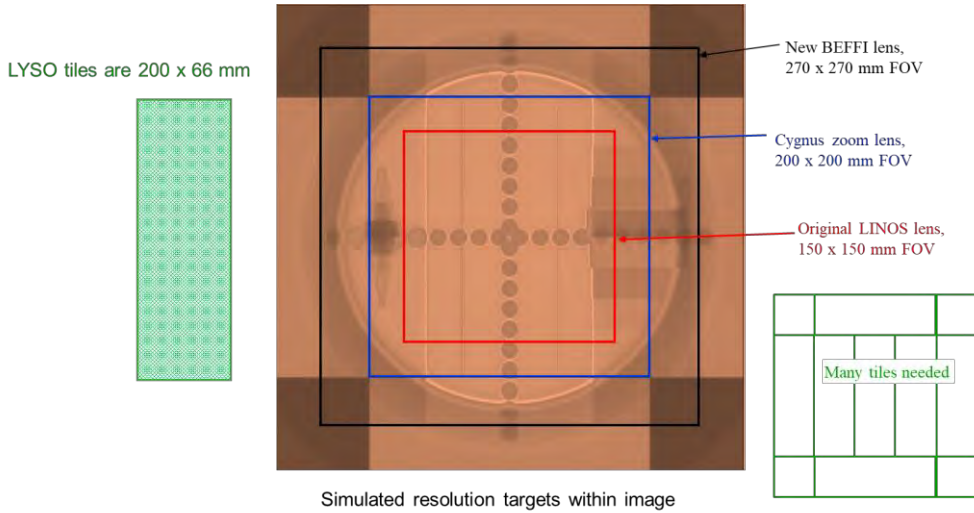


Figure 3. Evolution of LYSO scintillator constructions. Green boxes represent each LYSO tile measuring 200 x 66 mm.

Image in Figure 3 shows a simulated radiograph of a calibration scene with calibration markers and a radiographic object with steps of different thicknesses to provide a gradient of transmission for calibration purposes. The red square shows the FOV of the original LINOS lens at 150 × 150 mm. The blue square indicates the 200 × 200 mm FOV for the Cygnus zoom lens. The black square shows the 270 × 270 mm FOV of the new BEFFI lens. The scintillator “tiles” that make up the larger scintillator detector panel are outlined in green.

5. THE BEFFI LENS DESIGN

The design of the lens involves a carefully executed ray tracing process using CodeV software. In this process, the requirements for the lens are taken into consideration and are evaluated in conjunction with the optical qualities, size of the lens, and cost. Hundreds of configurations are considered and passed through global optimizations where many parameters are evaluated and iterated to a final optimized configuration. Best global optimizations are the ones that showed minimum ray bending at the optical surfaces. If a ray shows a sharp direction change when going into or out of a glass surface, tight tolerances for position of that optical element would be unreasonably high. Only a few configurations out of hundreds were carried into further design studies. The final design of the BEFFI lens incorporates 11 lens elements and is telecentric. As the LYSO scintillator light emission peaks at 435 nm, special glass types are required for the lens elements.

Telecentric lenses are designed to have a constant magnification regardless of the object’s distance from the lens or lateral location in the FOV. Telecentric design is utilized to provide high-resolution imaging with the thick monolithic detectors on Cygnus radiography. Thick monolithic scintillators are used at Cygnus due to the high 2.3 MeV endpoint

energy. Higher-energy x-rays interact throughout the entire thickness of the scintillator and laterally across the entire FOV. A non-telecentric lens like the original LINOS lens, shown in Figure 4a, collects light at an angle that is not perpendicular to the surface of the detector (blue arrows in Figure 4a). This results in an image with different magnifications from the different depths of the thick scintillator, introducing blurring to the image. This effect can also be understood as a limited depth of field. The telecentric lens system allows us to use thicker scintillators that are brighter for the typically light-starved dynamic experiments at Cygnus. Effective focal length of the LINOS lens is 160 mm. Effective focal length of the current Cygnus zoom lens varies from 805 to 1787 mm. The BEFFI lens effective focal length will vary from 1450 to 1500 mm.

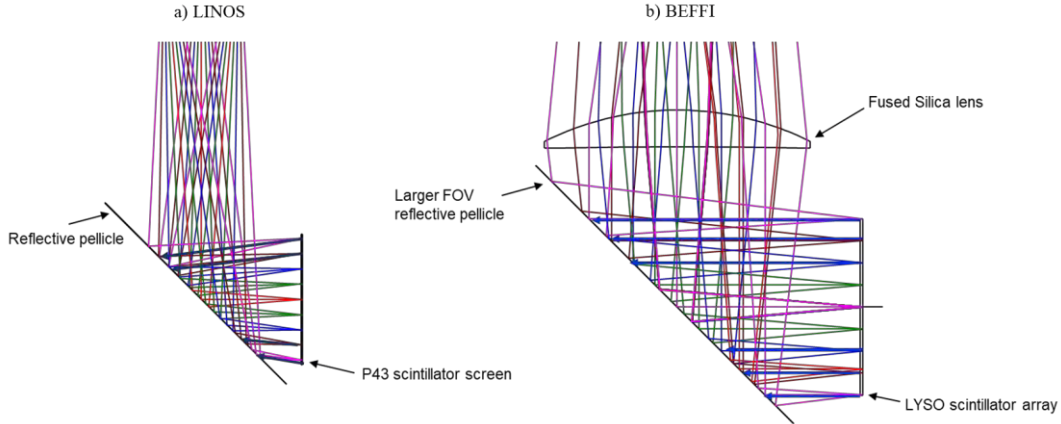


Figure 4. Optical rays collected by the LINOS lens are not parallel to the surface of the scintillator; some example rays are highlighted in blue. Using thick scintillators with the LINOS lens, will introduce blur to the image, affecting resolution and overall image quality. The BEFFI relay collects telecentric light.

Figure 5 shows which optical elements must move when we use the BEFFI lens system to zoom to different CCD image sizes. There are two moving doublet lenses. The stop plate must move, and its hole diameter is changed. The CCD with its vacuum window must move to support scintillators of different thicknesses and focusing activities (only the vacuum window of the CCD is shown).

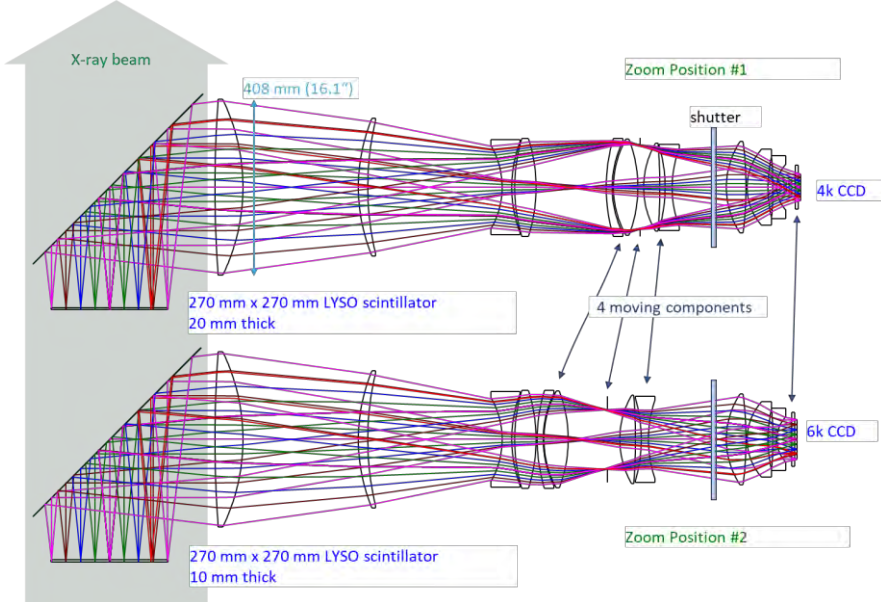


Figure 5. Optical elements that move when different CCD cameras are used with the BEFFI lens system are shown for the $4k \times 4k$ camera viewing a 20 mm thick LYSO scintillator (top) and the $6k \times 6k$ camera viewing a 10 mm thick LYSO scintillator (bottom).

Three different dual imaging configurations are being planned and are shown in figure 6. The dual scintillator imaging configuration shown in Figure 6B has two LYSO scintillator arrays, consisting of scintillators of different thicknesses, separated by approximately 60 cm. A BEFFI lens system with a $6k \times 6k$ camera would be the upstream camera and behind it a second BEFFI lens system with a $4k \times 4k$ camera. This configuration will be the first one to be used. The double-sided imaging configuration (Figure 6C) has only one LYSO scintillator array. The upstream camera records the image from one side of the scintillator, and the downstream camera records the image from the other side of the scintillator. The two recorded images will be combined into a single image with improved statistical uncertainties. If double-sided imaging is too complicated to setup, then the configuration shown in figure 6A will be used. The metal foil will prevent cross talk of the light between the two cameras. Many future experimental requirements need two identical images (same magnification) that can be combined to improve statistical accuracy of the intensities in the image.

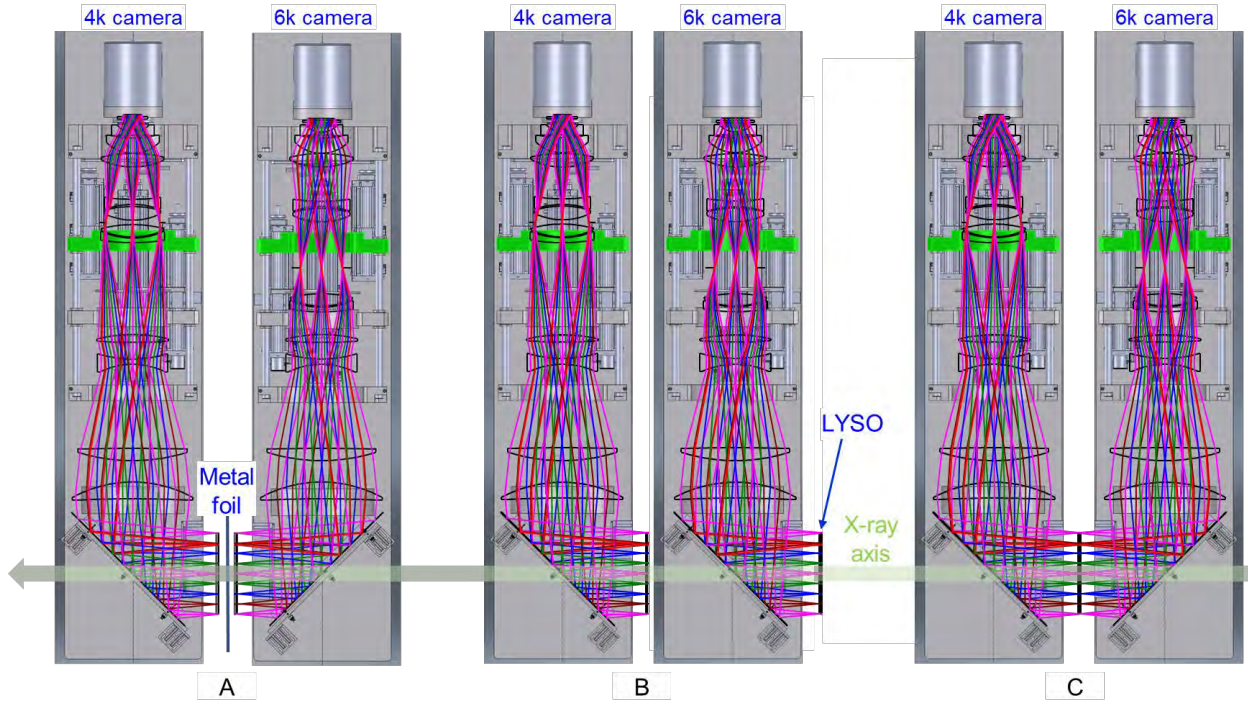


Figure 6. Three possible configurations for recording x-ray images onto two different cameras.

The BEFFI lens system has been designed to be able to use different cameras, with 61 mm square CCD or 92 mm square CCD, with a fixed FOV. The CZLS currently operates with the $4k \times 4k$ pixel 61 mm square CCD. The BEFFI lens is currently being planned to operate with a $6k \times 6k$ pixel camera with the 92 mm square CCD in the first camera down the Cygnus x-ray axis and a $4K \times 4k$ pixel 61 mm square CCD camera behind it for the second camera. The two imaging systems per Cygnus axis can accommodate different thickness scintillators. Flexibility in the BEFFI lens system also accommodates multiple detector configurations, which will provide advantages to the experiment depending on the configuration selected. This flexibility in the design of the new BEFFI lens system will allow us to successfully meet physics requirements for future SCEs and focused physics experiments.

When completed, two imaging systems will collect data from each of the two Cygnus x-ray beams. The four moving lens components and the complex underground environment require a high-level mechanical engineering of the lens housing. Four BEFFI lens systems will be installed vertically in the Cygnus zero room, two on each Cygnus axis. They get moved in and out of their nominal locations for vessel installation and alignment purposes, as well as other routine procedures in the zero room. The lenses also require fine alignment and focusing procedures, so the mechanical housing must be able to support the performance of these procedures. Figure 1 shows the two scintillator configurations in their mechanical enclosure, coupled with the lens and camera housing that will be installed vertically in the Cygnus zero room. The enclosure is light tight to avoid detecting any light from the exterior of the system. Each lens housing will

provide movement to the adjustable lens elements and will precisely align all the lenses with their center along a single axis. The mechanical design must also consider and dampen vibrations that are introduced to the system through the complex environment that surrounds it. As the system is prepared for execution, the optics and camera are carefully aligned, together with the scintillator detector panel, with millimeter precision. The mechanical housing and translation mechanisms of the lens system must allow this fine precision alignment, and ultimately maintain it as the system gets moved tenths of centimeters to support other zero room activities.

Upcoming experiments at the Cygnus testbed have physics requirements for object density reconstruction that call for high spatial resolution over a wide dynamic range of densities and across a large area of the scene. The BEFFI lens was carefully designed to meet these requirements. Figure 7 shows the modulation transfer functions for a range of field locations across the FOV from the center of the scintillator and progressively out to the edges of the scintillator where image quality falls due to the nature of how rays propagate through the lens system. Modulation transfer functions are widely used in optical design to show the performance of an optical system. They show how the contrast (modulation) varies as a function of spatial frequencies. In Figure 7, spatial frequencies have been transformed to a spatial dimension (the inverse of a spatial frequency) corresponding to a feature size. Modulation transfer functions are a quantitative metric for the spatial scale of features that will be resolved at a certain acceptable contrast level (typically 50% though many choose the acceptable contrast to be much lower) and guarantees that physics requirements can be met.

Physicists in charge of analyzing the x-ray data don't fully appreciate or know how to use the MTF charts. Normally optics programs only show the lp/mm resolutions at the camera. This is useful information for the optical lens designer. Nobody else makes good use of this scaling. So, we added a second line with the lp/mm resolutions at the LYSO scintillator. This is useful for someone setting up an Air Force resolution patterns in the object plane and measuring the overall image resolutions. This second axis sees more widespread use; but physicists were still confused on how to use the MTF charts. Lastly, we added a third scaling showing the feature resolution sizes. Now, the MTF curves have better meaning to all the stakeholders of the dynamic testing. Notice that the third horizontal axis scaling is non-linear. Changing from 1 lp/mm to 2 lp/mm changes the feature size by 1.5 mm. Changing from 19 lp/mm to 20 lp/mm changes the feature size by 0.008 mm. This will eliminate much of the confusion people have in making use of the MTF charts. Additionally, we find it more useful to change the y axis label from "Modulation" to "Image Contrast." This has more meaning to the Physicists.

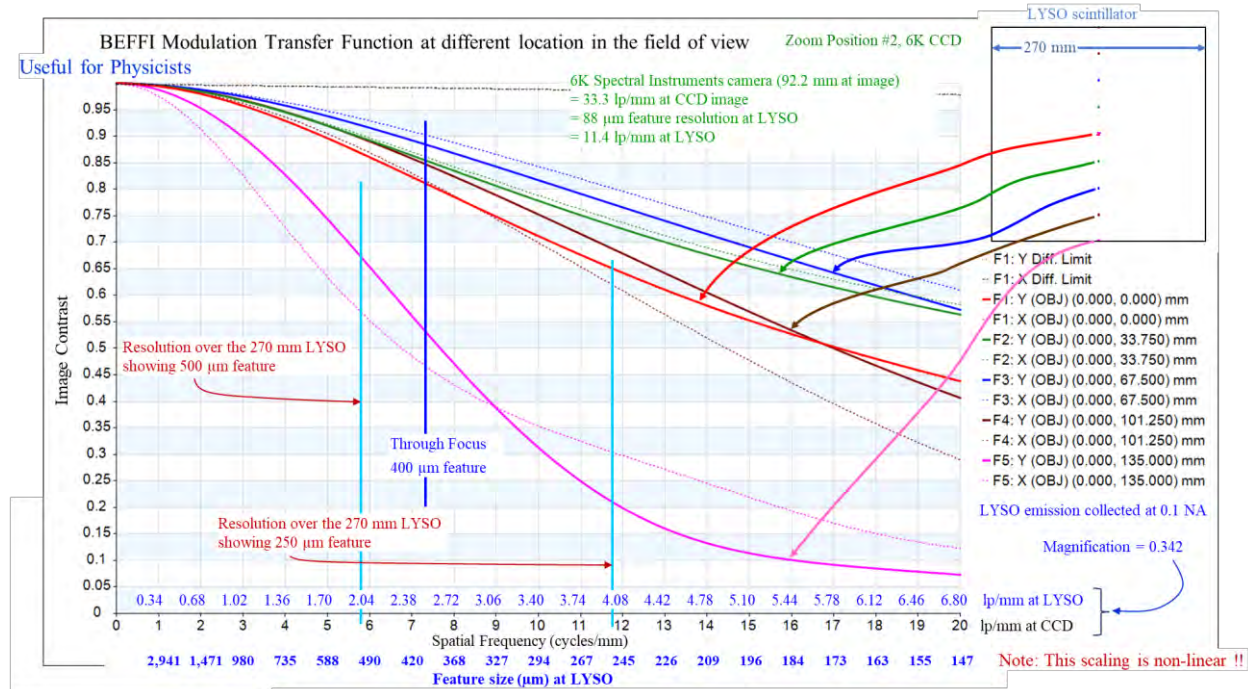


Figure 7. Modulation transfer functions are shown for five different field point locations from the scintillator (represented by red, green, blue, brown, and magenta dots on a 270 mm square in the top right corner of the plot).

The vertical light blue line in Figure 7 intersects the modulation transfer function at a value of 250-micron feature size at the scintillator plane. This region is of particular interest because it is close to the limiting resolution of monolithic LYSO scintillators due to the inherent physics of the scintillation process [6]. As high-energy x-rays interact with the LYSO scintillator crystal, recoil electrons are created from the interaction and travel a finite distance in the scintillator. As they travel in this transport phenomena, they cause ionization and undergo multiple Coulomb scattering events, losing their energy to the scintillation medium. The finite range of the high-energy electron in the scintillator results in a spread of energy deposited over a region of approximately 250 microns, which translates into the physical lower limit (sometimes called “physics blur”) of the resolution for a moderately thick LYSO scintillator. Inspecting the modulation transfer curves at this limiting detector resolution imposed by the scintillator physics provides information about the performance of the optical system at this key spatial dimension.

But realistically, we expect to resolve 500-micron features. This is because we are imaging from a volume light source. Through focus MTF of the 400-micron feature light from figure 7 is shown in figure 8. The 6K CCD will be collecting light from a 10 mm thick scintillator. However, the depth of field is about 4.5 mm total. To achieve this 400-micron feature sizes, the lens will have to be stopped down, which will reduce the amount of available light. Otherwise, larger feature resolution will have to be acceptable to the physicists conducting the experiments. We have plotted the defocusing scales at the CCD location as well as at the LYSO location. The difference between these two scales is magnification squared. Notice that when analyzing the locations of highest contrast for the different field points we see that the image plane has slight curvature. The flatness tolerance of the CCD chip is specified to be ± 20 microns.

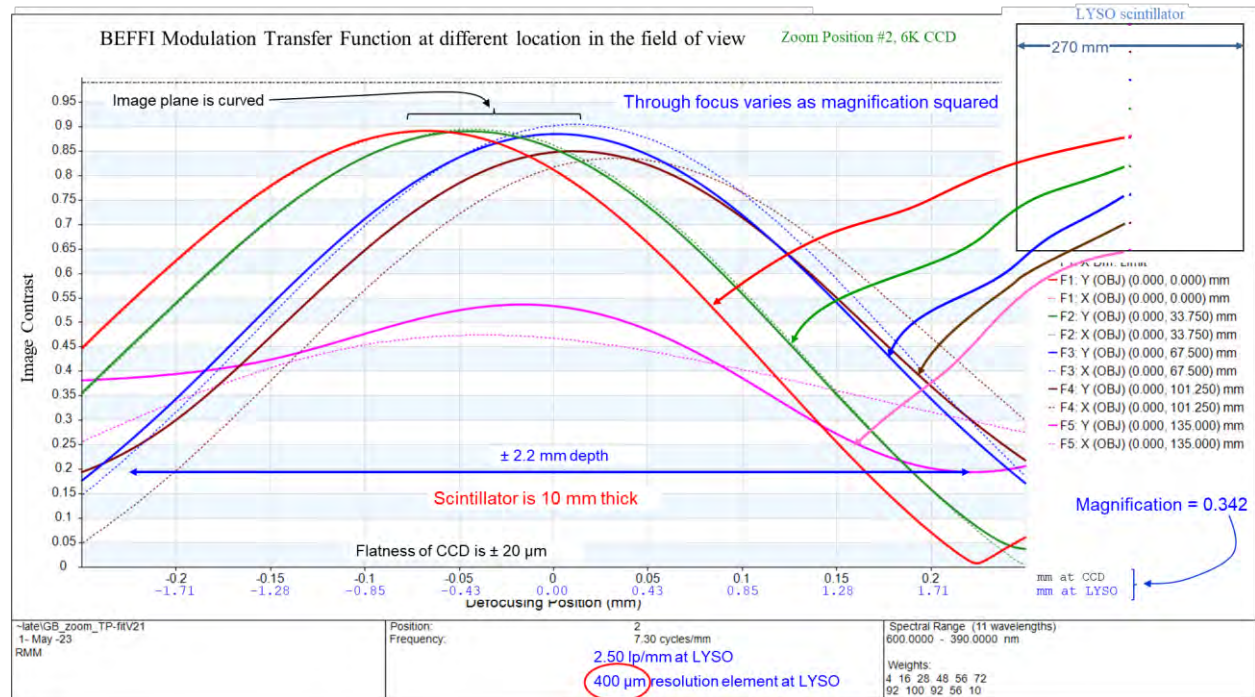


Figure 8. Through focus MTF shows that there is a limit to volume thickness of scintillator for a desired feature resolution.

The current Cygnus zoom lens design has an apparent barrel distortion, which was deemed acceptable as it was corrected in post-shot image restoration. However, using lessons learned from that design effort, the new lens has almost negligible distortion. Figure 9 shows the distortion grid of the Cygnus zoom lens on the left with up to 2.8%-barrel distortion and the distortion grid of the BEFFI lens on the right with a minor -0.42% pincushion distortion on the corners and -0.2% pincushion distortion in the center plane. The distortion in the Cygnus zoom lens images is very apparent by eye; barrel distortion is removed in data analysis with a code that was developed for this task. Distortion characterization images that were taken as part of the Cygnus zoom lens qualification process were used in the development of this code.

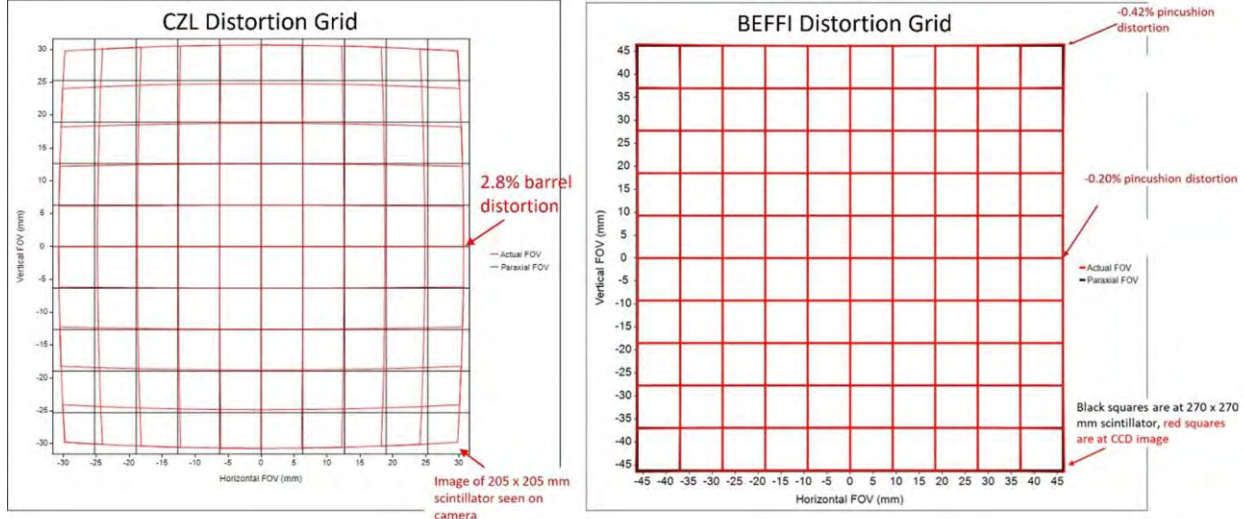


Figure 9. Comparison of distortion grids: the Cygnus zoom lens (left) and the new BEFFI lens (right).

Special calibration plates can be substituted for the tiled scintillator plate. Figure 10 shows one these plates used with a 20 mm thick scintillator. This calibration plate can swap positions with the scintillator. Alignment pins allow perfect registration of the different frames. There are different thicknesses of Sapphire placed on top of Air Force resolution patterns. Sapphire has nearly the same index of refraction as the LYSO scintillator. Using this calibration plate, the experimenter will establish the correct plane to focus upon within the LYSO scintillator. This calibration plate allows equalization of astigmatism in the image by adjusting the tilt of the CCD camera and decentering a compensator doublet within the zoom lens system. Other calibration plates will present a grid to the camera to provide distortion measurements, used to analyze the images.

Figure 11 shows that much baffling is needed to eliminate unwanted light from getting into the camera. The LYSO scintillator emits light into wide angles. Only a few percent of this light can be used to form images. If more depth of field is needed to resolve a feature size, then the stop diameter must be reduced. Notice that different stop diameters will be sifted to different distances, because the stop surface is curved.

Care must be taken when viewing both the front side and the back side of the same scintillator. If the AR coating on the CCD chip is not good enough, it will reflect some light backwards through the transparent scintillator and into the second camera. Figure 12 shows several flat field images that demonstrated that unwanted stray light could occur if good AR coatings are now applied to the CCD chip. Images collected by other cameras did not show this unwanted feature. The example of figure 12 was done using other lenses and other cameras. If a particular camera must be used and both CCD camera must have the same magnification, then the configuration shown in figure 6a will be used. Here, a thin metal foil will block the unwanted light.

Sapphire has almost the same index as the LYSO scintillator. At 435 nm, LYSO index is 1.824. At 435 nm, Sapphire index is 1.782.

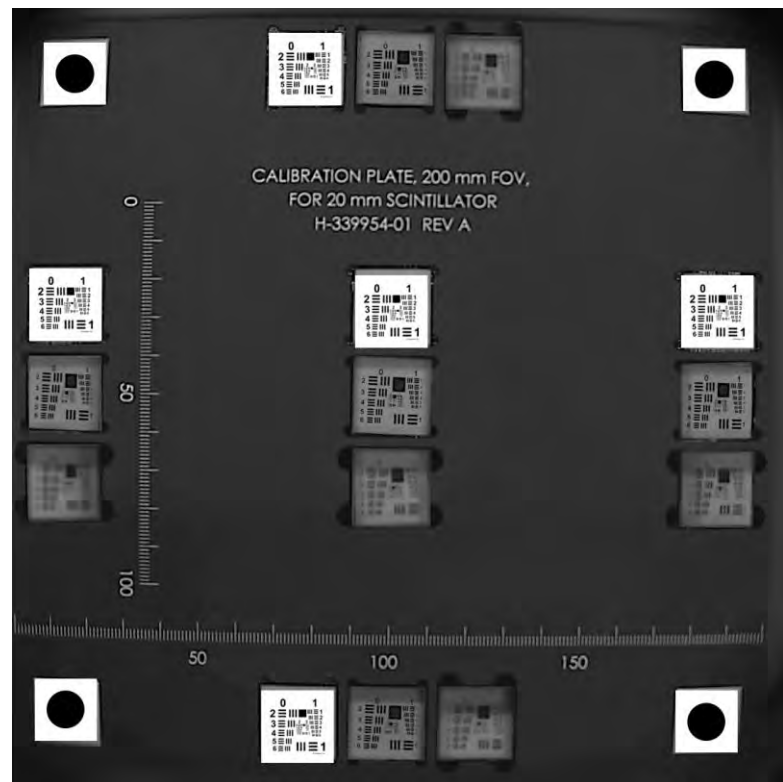


Figure 10. Example of a calibration target for setting focus within a volume scintillator.

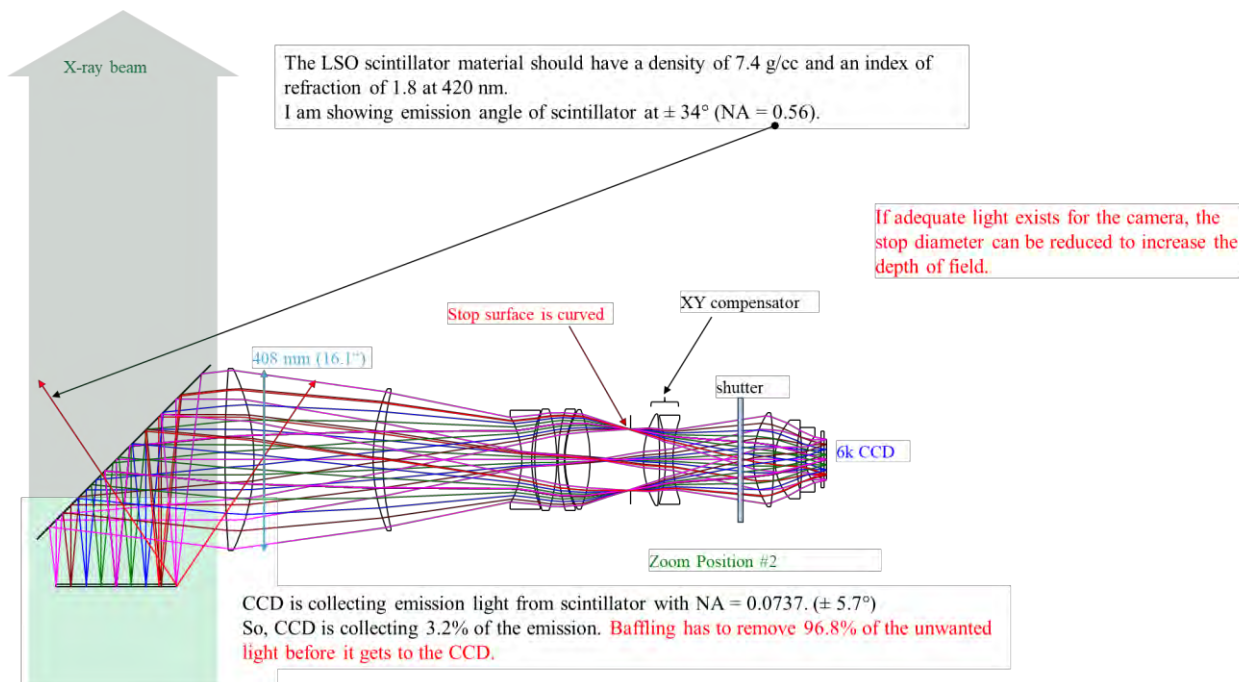
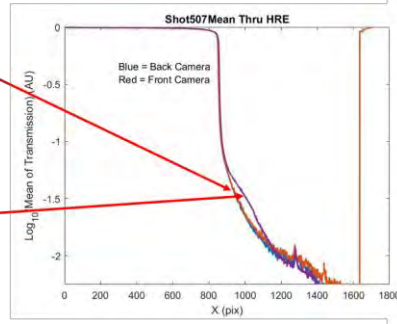
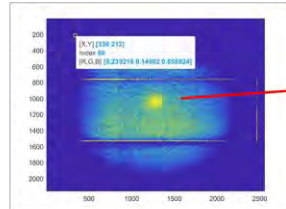


Figure 11. Different stop diameters can be used to adjust the depth of field, used for different scintillator thicknesses.

“Spot” Feature

► Line-outs moved below the feature



Shots 499-501 are flat fields for double-sided imaging that shows this feature scatters light

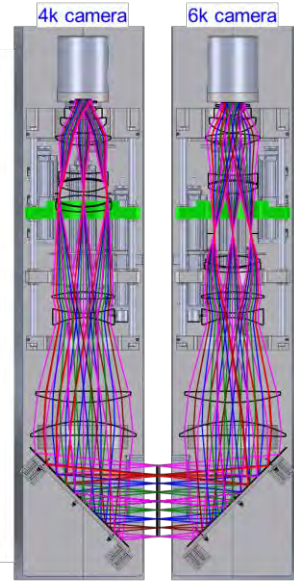
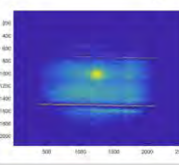
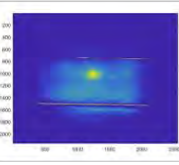
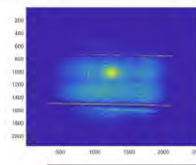


Figure 12. Several flat field calibration images of double-sided imaging showed a 1-2% stray light feature in the imaging on one of the cameras. The other camera did not show this 1-2% stray light feature. This data was taken using other cameras and other lenses; but on the new BEFFI lens system.

6. CONCLUSIONS

Dual scintillator imaging has many advantages. Having a thicker scintillator captures an areal density dynamic range that is shifted toward denser objects. If the LYSO scintillators are arranged serially, the rear downstream camera would capture a similar areal density dynamic range at a slightly different radiographic magnification. In this scenario, the image from the rear camera provides complementary information that allows a continuous reconstruction of the density profile across scintillator tile boundaries.

The BEFFI lens systems will replace all four lens systems at the Cygnus Dual Beam Radiographic Facility, replacing two Cygnus zoom lens systems and two LINOS lens systems (shown in figure 1). It will provide the largest FOV ever collected at Cygnus and record high-resolution images with even contrast across the entire FOV. The BEFFI lens also provides flexibility in accommodating different scintillator detector configurations that have specific advantages and can be chosen depending on the requirements of the experiment.

Volume source imaging requires a telecentric imaging systems. Pulsed x-ray imaging is usually light starved. There is a trade-off between depth of field within the volume scintillator and having enough photons (changing the stop diameter) for adequate statistics in the image. Thus, there will always be a trade off between having adequate light for recording of the images and recording the smallest acceptable feature sizes within a volume scintillator.

ACKNOWLEDGMENTS

This manuscript has been authored by Mission Support and Test Services, LLC, under Contract No. DE-NA0003624 with the U.S. Department of Energy, National Nuclear Security Administration, Office of Defense Programs. The United States Government retains and the publisher, by accepting the article for publication, acknowledges that the United States Government retains a non-exclusive, paid-up, irrevocable, worldwide license to publish or reproduce the published form of this manuscript, or allow others to do so, for United States Government purposes. The U.S. Department of Energy will provide public access to these results of federally sponsored research in accordance with the DOE Public Access Plan (<http://energy.gov/downloads/doe-public-access-plan>). The views expressed in the article do not necessarily represent the views of the U.S. Department of Energy or the United States Government. DOE/NV/03624--1777.

REFERENCES

- [1] Weidenheimer, E., Corcoran, P., Altes, R., Douglas, J., Nishimoto, H., Smith, I., Stevens, R., Johnson, D. L., White, R., Gustwiller, J., Maenchen, J. E., Menge, P., Carlson, R., Fulton, R. D., Cooperstein, G., Junt, D., "Design of a driver for the Cygnus X-ray source," Pulsed Power Plasma Science, PPPS-2001, **1**, 591-595 (2001).
- [2] Smith, J., Carlson, R., Fulton, R., Chavez, J., Coulter, W., Gibson, W., Helvin, T., Henderson, D., Mitton, V., Ormond, E., Ortega, P., Ridlon, R., Vallerio, A., "Performance of the Cygnus X-ray source," 29th IEEE International Conference on Plasma Science, ICOPS 2002, p. 326 (2002).
- [3] Malone, R.M., Baker, S.A., Brown, K. K., Curtis, A. H., Esquibel, D. L., Frayer, D. K., Frogget, B. C. Furlanetto, M. R., Garten, J. R., Haines, T. J., Howe, R. A., Huerta, J. A., Kaufman, M. I., King, N. S. P., Lutz, S. S., McGillivray, K. D., and Smith, A. S., "Design and assembly of a telecentric zoom lens for the Cygnus x-ray source," Proc. SPIE 8488, 116-129, (2012), DOI: 10.1117/12.929160
- [4] Malone, R. M., Baker, S.A., Brown, K. K., Castaneda, J. J., Curtis, A. H., Danielson, J., Droemer, D. W., Esquibel, D. L., Haines, T. J., Hollabaugh, J. S., Howe, R. A., Huerta, J. A., Kaufman, M. I., King, N. S. P., Lutz, S. S., McGillivray, K. D., Smith, A. S., Stokes, B. M., and Tibbitts, A., "Alignment and testing of a telecentric zoom lens used for the Cygnus x-ray source," Proc. SPIE 8844, 88440A (2013); DOI:10.1117/12.2022768
- [5] Smalley, D. D., Duke, D., Webb, T., Baker, S.A., Castaneda, J. J., Corredor, A. C., Danielson, J., Gehring, M., Haines, T. J., Lutz, S. S., Montoya, K., and Stearns, J., "High-energy radiographic imaging performance of LYSO," *Nucl. Instrum. Methods Phys. Res. A* 914, pp. 57–63 (January 11, 2019), DOI: 10.1016/j.nima.2020.163910.
- [6] Smalley, D. D., Baker, S. A., Baldonado, B. J., Castaneda, J. J., Corredor, A. C., Clayton, J. H., Fegenbush, L., Gautier, C., Gehring, A., Haines, T. J., Lucero, J., Sterns, J., and Walters, K. L, "Image restoration of high-energy X-ray radiography with a scintillator blur model," *Nucl. Instrum. Methods Phys. A* 968, 163910 (July 11, 2020), DOI: 10.1016/j.nima.2020.163910.